

# HIGHER-POINT FUNCTIONS IN $\mathcal{N} = 4$ SYM FROM AN INTEGRABLE SYSTEM\*

B. EDEN

Institute of Mathematics, Humboldt-University Berlin  
Zum großen Windkanal 2, 12489 Berlin, Germany

*Received 22 February 2023, accepted 22 February 2023,  
published online 25 May 2023*

We review how structure constants in  $\mathcal{N} = 4$  super Yang–Mills theory in four dimensions can be computed using an integrable system. Then we present our generalisation of the formalism to higher-point functions of gauge-invariant composite operators of the model. We conclude by listing achievements and future directions.

DOI:10.5506/APhysPolBSupp.16.5-A30

## 1. Introduction: Review of AdS/CFT integrability

The  $\mathcal{N} = 4$  model is the maximally supersymmetric non-Abelian gauge theory in four dimensions. We assume gauge group  $SU(N)$  in a large- $N$  limit. The super-partners of the field strength are four massless Majorana–Weyl fermions and three massless complex scalar fields. All of these transform in the adjoint representation of the gauge group. The theory is conformally-invariant also at the quantum level, which becomes most transparent in configuration space.

Gauge-invariant composite operators are given by products of the fields under a gauge group trace. Simple examples are

$$\mathcal{O}_L = \frac{1}{\sqrt{LN^L}} \text{Tr} (X^L) , \quad \mathcal{O}_L^k = \text{Tr} \left( X^{L-k-2} Y X^k Y \right) , \quad Y \neq X, X^* . \quad (1)$$

The *half-BPS operators*  $\mathcal{O}_L$  are finite, *i.e.* do not have anomalous dimension. On the other hand, the *BMN operators* [1]  $\mathcal{O}_L^k$  with many  $X$ s and two scalar *excitations*  $Y$  must be renormalised. They are *a priori* not conformal eigenoperators so we obtain a large mixing problem for every *length*  $L$ .

---

\* Presented at the Diffraction and Low- $x$  2022 Workshop, Corigliano Calabro, Italy, 24–30 September, 2022.

A two-point function of BMN operators receives a one-loop correction only from the superpotential vertex, see Fig. 1. The Wick contraction of the vertex on the first operator defines a linear map whose eigenvalues are the anomalous dimensions. By way of example, at length 4, the operator basis has just the two members  $\{\mathcal{O}_4^0, \mathcal{O}_4^1\}$ . The mixing matrix is

$$\Gamma_1/N = \begin{pmatrix} 2 & -4 \\ -2 & 4 \end{pmatrix} \quad (2)$$

and has eigenvalues/eigenvectors

$$\gamma_{1,0} = 0, \quad \underline{v}_0 = 2\mathcal{O}_4^0 + \mathcal{O}_4^1, \quad \gamma_{1,1} = 6, \quad \underline{v}_1 = \mathcal{O}_4^0 - \mathcal{O}_4^1. \quad (3)$$

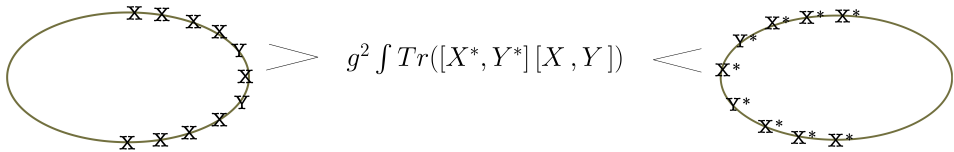


Fig. 1. A two-point function of BMN operators in position space. Spectator propagators (not involved in the interaction) are omitted.

Restricting to *single-trace operators* and *planar graphs* enforces a nearest neighbour interaction. Identifying  $X = \downarrow$ ,  $Y = \uparrow$ , we obtain a *circular spin chain* with the *Hamiltonian*  $H = \mathbb{I} - \mathbb{P}$  owing to the commutators in the four-vertex [2], the *Heisenberg chain*. The *Bethe ansatz* yields its eigenenergies: every excitation moves along the chain with a quasi-momentum/rapidity  $2u = \cot(p/2)$ . These must obey the *Bethe equations*

$$e^{ip_j L} \prod_{k \neq j} S_{jk} = 1, \quad S_{jk} = \frac{u_j - u_k - i}{u_j - u_k + i}, \quad (4)$$

with the *free propagation phase*  $e^{ip_j L}$  and the *scattering matrix*  $S$ . Importantly, there is *factorised scattering*: multi-particle scattering factorises into two-particle processes. In addition, by the cyclicity of the gauge group trace  $\sum_i p_i = 0$ .

In the  $L = 4$  example, we find  $u_2 = 1/\sqrt{12} = -u_1$  with energy

$$\gamma_1 = \sum_{i=1}^2 \frac{1}{u_i^2 + \frac{1}{4}} = 6. \quad (5)$$

It is possible to generalise the spin-chain model to a more complete set of excitations and to include the effect of higher-loop Feynman diagrams

changing to the so-called Zhukowsky variable  $x^\pm(u, g^2 N / (8\pi^2))$  and introducing a certain phase factor [3, 4]. The resulting *asymptotic all-loops Bethe equations* are valid as long as the loop order does not exceed the operator length. At higher orders, *finite-size corrections* become relevant [5].

In Fig. 2, we depict a three-point function of single-trace operators, or equivalently, a three-string vertex. An integrable systems approach to three-point computations has been devised in [6]. The three-vertex is split into its back and front surface yielding hexagonal patches. In the figure, the *virtual edges* are coloured. These correspond to bunches of propagators stretching between the operators. The *physical edges* representing single-trace operators are marked in black.

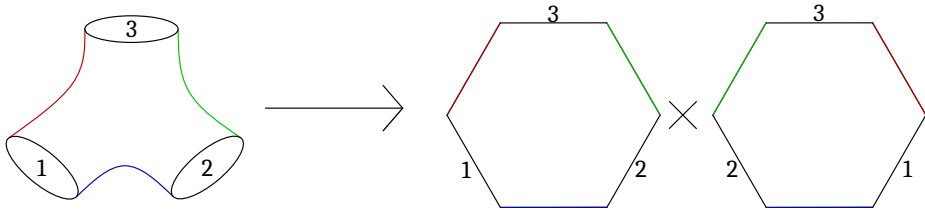


Fig. 2. Splitting a three-point function into two hexagons.

The operators also have to be split, taking into account all distributions of excitations or *magnons*

$$\begin{aligned} \psi_{\{Y_1, Y_2\}}^{l_1+l_2} &\equiv \psi_{\{Y_1, Y_2\}}^{l_1} \psi_{\{Y_2\}}^{l_2} + e^{i p_2 l_1} \psi_{\{Y_1\}}^{l_1} \psi_{\{Y_2\}}^{l_2} \\ &+ e^{i p_1 l_1} S_{12} \psi_{\{Y_2\}}^{l_1} \psi_{\{Y_1\}}^{l_2} + e^{i(p_1+p_2)l_1} \psi_{\{Y_1\}}^{l_1} \psi_{\{Y_1, Y_2\}}^{l_2}, \end{aligned} \quad (6)$$

where the symbol  $\psi_{\{\dots\}}^l$  denotes a Bethe state of length  $l$  with a given set of magnons. The shift operator and  $S$  matrix are as in (4). The total hexagon amplitude is then

$$\mathcal{A} = \sum_{\alpha \cup \bar{\alpha} = \{u_i\}} w(\alpha, \bar{\alpha}) (-1)^{|\alpha|} \mathfrak{h}_{Y \dots Y}(\alpha) \mathfrak{h}_{Y \dots Y}(\bar{\alpha}), \quad (7)$$

where  $\alpha, \bar{\alpha}$  denote the *partition* of the set of magnons into two subsets and the *splitting factors*  $\omega$  can be inferred from (6). The individual hexagon is evaluated as follows: as in the all-loops spectrum problem the excitations are represented as  $\chi^{AA'} = \chi^A \otimes \bar{\chi}^{A'}$ . In particular, we write  $Y = \phi^1 \otimes \bar{\phi}^{2'}$  and arrange all  $\phi$ s on a *left* and all  $\bar{\phi}$ s on a *right chain*. In the hexagon approach, scattering takes place on one of the chains, no matter which

$$\mathfrak{h}_{Y_1 \dots Y_n} = \left( \prod_{j < k} \frac{u_j - u_k}{u_j - u_k - i} \right) \left\langle \phi_n^1 \dots \phi_1^1 \middle| \mathbb{S} \middle| \bar{\phi}_1^{2'} \dots \bar{\phi}_n^{2'} \right\rangle. \quad (8)$$

For instance, for three  $Y$  excitations (or *magnons*),

$$\mathbb{S} \left| \bar{\phi}_1^{2'} \bar{\phi}_2^{2'} \bar{\phi}_3^{2'} \right\rangle = S_{12} S_{13} S_{23} \left| \bar{\phi}_3^{2'} \bar{\phi}_2^{2'} \bar{\phi}_1^{2'} \right\rangle. \quad (9)$$

Finally, bra- and ket-state are contracted employing the rule  $\langle \phi_j^a | \bar{\phi}_j^{b'} \rangle = \epsilon^{ab'}$ . Again, in an asymptotic regime, corrections in the 't Hooft coupling can be incorporated by  $x^\pm$  and the phase factor [4, 6].

While *finite-size effects* become relevant to the spectrum problem only at four loops and beyond, they can enter into the structure constant computation already at  $O(g^2)$ . To compute these, we have to insert *bound states*  $B_a$  in *mirror kinematics* ( $x^+(u) \rightarrow 1/x^+(u)$  or  $x^-(u) \rightarrow 1/x^-(u)$ )

$$\delta \mathcal{A} = \sum_{a>0} \int \frac{du}{2\pi} \mu(u) \omega(\alpha, \bar{\alpha}) \mathfrak{h}_{BY\dots Y}(u^\gamma, \alpha) \mathfrak{h}_{Y\dots Y\bar{B}}(\bar{\alpha}, u^{-\gamma}) \quad (10)$$

( $\gamma$  denotes the type of rotation, cf. [6]) on the virtual edges. This can be interpreted as *gluing* the cut edges by the insertion of one (or several) *virtual magnons*. The last formula contains the *mirror measure*

$$\mu(u) = \frac{a (g^2)^{l_{ij}+1}}{(2 u^+ u^-)^{l+2}} + \dots, \quad u^\pm = u \pm i \frac{a}{2}. \quad (11)$$

The *edge width* or *bridge length*  $l_{ij} = (L_i + L_j - L_k)/2$  thus determines the loop order at which such corrections start to contribute.

## 2. Soft cushions — BMN-(BPS)<sup>3</sup> four-point functions

Consider planar  $SU(N)$  four-point tree diagrams in position space. The single-trace operators have to be connected on the surface of a sphere. Parallel propagators between points  $i, j$  form one edge of width  $\{l_{ij}\}$ .

Let us place a BMN operator (1) at point 1 and half-BPS operators at the other ends. Looking onto point 1, we recognise hexagons — three in the first two graphs of Fig. 3 (the bottom one between points 2,3,4 does

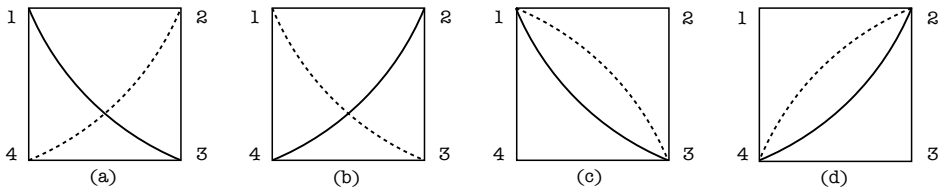


Fig. 3. The four classes of planar four-point graphs (dashed lines behind the plane of the drawing).

not carry excitations and is therefore trivially equal to 1), and even four in the third panel. The fourth diagram will not come into play in our set of examples. We have to iterate the partitioning: in the first panel of Fig. 4, let us initially place both excitations on the hexagon 1,2,3 and migrate them over the edge 13, finally 14. The second panel requires a triple partition. Partition invariance is guaranteed by the Bethe equations.

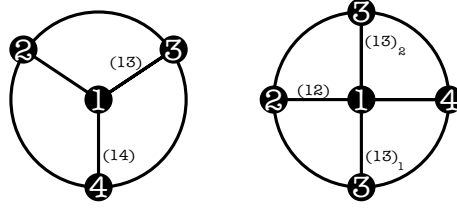


Fig. 4. Panels (a) and (c) of Fig. 3 looking onto point 1.

By conformal transformations, any three points can be moved onto a line. The *twisted translation* of the hexagon formalism mixes the fields in relation to their position along this axis. This results in the effective propagators  $\langle X(a_1)X(a_2) \rangle = 1$ ,  $\langle Y(a_1)X(a_2) \rangle = 1/(a_1 - a_2)$ . Computing with these, we expect results homogeneous of the order of  $-2$  in  $a_1 - a_j$ . Choosing  $a_1 = 0$ , independent variables are *e.g.*  $a_{23} = 1/a_2 - 1/a_3$ ,  $a_{34} = 1/a_3 - 1/a_4$ .

There are no two-excitation BMN eigenoperators with  $\gamma_1 \neq 0$  at  $L < 4$ , one at length 4 or 5, and there are two at lengths 6 and 7. We denote these by 4, 5,  $6^\mp$ ,  $7'$ ,  $7''$  and also label the half-BPS operators by their lengths. For up to 7 Wick contractions [7]:

	$c$	$\underline{v}$		$c$	$\underline{v}$
$G(4; 222)$	$4\sqrt{\frac{2}{3}}$	(1,1,1)	$G(4; 242)$	$\frac{8}{\sqrt{3}}$	(1,0,1)
$G(4; 233)$	$\sqrt{6}$	(2,2,3)	$G(5; 232)$	$\sqrt{6}$	(3,2,3)
$G(6^\mp; 222)$	$4\sqrt{2}$	(1,1,1)	$G(4; 235)$	$\sqrt{10}$	(2,4,5)
$G(4; 244)$	$8\sqrt{\frac{2}{3}}$	(1,1,2)	$G(4; 343)$	$2\sqrt{3}$	(3,2,3)
$G(5; 252)$	$3\sqrt{10}$	(1,0,1)	$G(5; 234)$	$2\sqrt{3}$	(3,4,7)
$G(5; 333)$	$9\sqrt{6}$	(1,1,1)	$G(6^\mp; 242)$	$\frac{4(1\pm\sqrt{5})}{\sqrt{5}}$	(2,1,2)
$G(6^\mp; 233)$	$\frac{3(1\pm\sqrt{5})}{\sqrt{10}}$	$(4, 4, 6 \pm \sqrt{5})$	$G(7'; 232)$	$2\sqrt{6}$	(2,1,2)
$G(7''; 232)$	$6\sqrt{2}$	(1,1,1)			

where

$$G(\dots) = c * \underline{v} \cdot (a_{23}^2, a_{23}a_{34}, a_{34}^2) . \quad (12)$$

Introducing an orbital part for the hexagon

$$\mathfrak{h}_{1ij}(\alpha) \rightarrow \widehat{\mathfrak{h}}_{1ij}(\alpha) = (a_{ij})^{|\alpha|} \mathfrak{h}_{1ij}(\alpha), \quad a_{ij} = \frac{1}{a_i} - \frac{1}{a_j}, \quad (13)$$

the sum of hexagon amplitudes for every set of edge widths on the graphs in Fig. 3 (a),(b),(c) (avoiding overcounting) exactly reproduces the table, if scaled up with a factor  $\sqrt{L_1 L_2 L_3 L_4}$  [7].

A more advanced test is the one-loop correction to the four-point functions of half-BPS operators, which is entirely carried by finite-size corrections [8]. The integrability computation directly matches Feynman graphs [9]

$$\int d\mu(v^\gamma) \left[ \text{Hexagon with } v^{-\gamma} \text{ and } v^\gamma \right] = \int d\mu(v^\gamma) \left[ \text{Hexagon with } v^{-\gamma} \text{ and } v^\gamma \right] = \frac{1}{2} \left( \text{Box with red wavy line} + \text{Box with red vertical line} \right)$$

Fig. 5. One magnon gluing as Yang–Mills exchanges between matter lines. Up to rational factors, the result is the off-shell one-loop box integral.

### 3. Conclusions

Hexagon tessellations compute flavour and combinatorics in tree-level  $\mathcal{N} = 4$  correlators. Colour factors must be imported into higher-point functions. Tilings can then address non-planar corrections, multi-trace operators, and the gauge groups  $U(N)$ ,  $SO(N)$ ,  $USp(N)$  [9]. On the other hand, at higher-loop orders, the interplay between Feynman graphs and gluing corrections is quite non-trivial so attributing the correct colour factors will be complicated. Last, in the hexagon tessellation scenario, we are currently using an  $S$ -matrix picture. The computation of higher-loop contributions from gluing is then a formidable problem. The sum-integrals obtained are akin to highly nested Mellin–Barnes representations.

### REFERENCES

- [1] D. Berenstein, J. Maldacena, H. Nastase, *J. High Energy Phys.* **2002**, 013 (2002).
- [2] J. Minahan, K. Zarembo, *J. High Energy Phys.* **2003**, 013 (2003).
- [3] N. Beisert, M. Staudacher, *Nucl. Phys. B* **727**, 1 (2005).
- [4] N. Beisert, B. Eden, M. Staudacher, *J. Stat. Mech.* **0701**, P01021 (2007).
- [5] Z. Bajnok, R. Janik, *Nucl. Phys. B* **807**, 625 (2009).
- [6] B. Basso, S. Komatsu, P. Vieira, [arXiv:1505.06745 \[hep-th\]](#).
- [7] B. Eden, A. Sfondrini, *J. High Energy Phys.* **2017**, 098 (2017).
- [8] T. Fleury, S. Komatsu, *J. High Energy Phys.* **2017**, 130 (2017).
- [9] B. Eden, Y. Jiang, D. le Plat, A. Sfondrini, *J. High Energy Phys.* **2018**, 170 (2018).